Electronic Supplementary Material (ESI) for Chemical Communications

Enhancement of CO_2 selectivity in a pillared pcu MOM platform through pillar substitution

Patrick Nugent, Vanessah Rhodus, Tony Pham, Brant Tudor, Katherine Forrest, Lukasz Wojtas, Brian Space and Michael Zaworotko

Supplementary Material

Materials and Methods

All reagents and solvents are commercially available and were used without further purification.

Single crystal X-ray diffraction data for **TIFSIX-1-Cu** and **SNIFSIX-1-Cu** were collected on a Bruker-AXS SMART APEX/CCD diffractometer using CuKα radiation (λ = 1.5418 Å, T = 228(2) K). Indexing was performed using APEX2.[1] Data integration and reduction were completed using SaintPlus 6.01.[2] Absorption correction was performed by the multi-scan method implemented in SADABS.[3] Space groups were determined using XPREP implemented in APEX2.[1] Structures were solved with SHELXS-97[5-7] (direct methods), and refined on F^2 using nonlinear least-squares techniques with SHELXL-97 contained in APEX2,WinGX v1.70.01,[4-7] and OLEX2 v1.1.5[8] program packages. All non-hydrogen atoms were refined anisotropically. The Ti-F bond distances for disordered F atoms in **TIFSIX-1-Cu** were refined using restraints. The pyridyl rings in both structures were disordered over two positions. For both structures the contribution of disordered solvent molecules was treated as diffuse using the Squeeze routine implemented in Platon.[9,10]

1. Bruker (2010). (APEX2). Bruker AXS Inc., Madison, Wisconsin, USA.
2. Bruker (2009). SAINT.Data Reduction Software.Bruker AXS Inc., Madison, Wisconsin, USA.
3. Sheldrick, G. M. (2008). SADABS.Program for Empirical Absorption Correction. University of Gottingen, Germany.
4. Farrugia, L. *J. Appl. Cryst*. 1999, **32**, 837.
5. Sheldrick, G.M. (1997) SHELXL-97. Program for the Refinement of Crystal.
6. Sheldrick, G. M. *ActaCryst*. 1990, **A46**, 467.
7. Sheldrick, G. M. *ActaCryst*. 2008, **A64**, 112.
8. O. V. Dolomanov, L. J. Bourhis, R. J. Gildea, J. A. K. Howard and H. Puschmann, *J. Appl. Crystallogr*., 2009, **42**, 339.
9. T. L. Spek, *ActaCryst*. 1990. **A46**, 194.
10. T. L. Spek, *ActaCryst.* 1990. **A46**, c34.

Powder X-ray diffraction (PXRD) was carried out at room temperature on a Bruker D8 Advance θ/2θ diffractometer using Cu-Kα radiation (λ = 1.5418 Å). 2θ scans between 3° and 40° with a step size of 0.02° were performed for a duration of 30 minutes.

Gas adsorption measurements were conducted on a Micromeritics ASAP 2020 surface area and porosity analyzer. Prior to data collection, **TIFSIX-1-Cu** and **SNIFSIX-1-Cu** were exchanged with methanol 3 times daily for 2 days and degassed under high vacuum at room temperature for 16 hours.

Preparation of $[Cu(bipy)_2(TiF_6)]$, TIFSIX-1-Cu: In a small test tube, 0.15 mmol (23.4 mg) of 4,4'-bipyridine in 3 mL of methanol was layered onto 3 mL of an ethylene glycol solution containing 0.076

mmol (17.7 mg) of $Cu(NO_3)_2 \cdot 2.5H_2O$ and 0.076 mmol (15.0 mg) of $(NH_4)_2TiF_6$. Purple plate-shaped crystals formed in 90.2% yield after 2 weeks.

Preparation of $[Cu(bipy)_2(SnF_6)]$, SNIFSIX-1-Cu: In a small test tube, 0.11 mmol (17.2 mg) of 4,4'-bipyridine in 3 mL of methanol was layered onto 3 mL of an ethylene glycol solution containing 0.056 mmol (13.0 mg) of $Cu(NO_3)_2 \cdot 2.5H_2O$ and 0.056 mmol (15.1 mg) of $(NH_4)_2SnF_6$. Purple plate-shaped crystals formed in 93.8% yield after 2 weeks.

Supplementary Data Tables

Table S1. Crystallographic Data for **TIFSIX-1-Cu** and **SNIFSIX-1-Cu**.

Compound	**TIFSIX-1-Cu**	**SNIFSIX-1-Cu**
Empirical formula	$C_{20}H_{16}CuF_6N_4Ti$	$C_{20}H_{16}CuF_6N_4Sn$
Formula weight	537.81	608.60
Temperature/K	228(2)	228(2)
Crystal system	tetragonal	tetragonal
Space group	P4/mmm	P4/mmm
a/Å	11.1001(6)	11.116(5)
b/Å	11.1001(6)	11.116(5)
c/Å	8.4055(7)	8.627(5)
α/°	90.00	90.00
β/°	90.00	90.00
γ/°	90.00	90.00
Volume/Å^3	1035.66(12)	1066.0(9)
Z	1	1
ρcalc/mg/mm^3	0.862	0.948
m/mm^{-1}	2.593	5.587
F(000)	269.0	297.0
Crystal size/mm^3	0.02 × 0.02 × 0.01	0.02 × 0.02 × 0.01
2Θ range for data collection	10.52 to 132.64°	7.96 to 133.06°
Index ranges	$-13 \le h \le 13$, $-9 \le k \le 12$, $-9 \le l \le 8$	$-13 \le h \le 12$, $-12 \le k \le 12$, $-9 \le l \le 10$
Reflections collected	5175	5235
Independent reflections	573[$R_{(int)}$ = 0.0698]	603[$R_{(int)}$ = 0.0557]
Data/restraints/parameters	573/3/48	603/0/40
Goodness-of-fit on F^2	1.054	1.188
Final R indexes [I>=2σ (I)]	R_1 = 0.0362, wR_2 = 0.1083	R_1 = 0.0317, wR_2 = 0.0732
Final R indexes [all data]	R_1 = 0.0385, wR_2 = 0.1095	R_1 = 0.0328, wR_2 = 0.0748
Largest diff. peak/hole / e Å^{-3}	0.36/-0.39	0.69/-0.81

Table S2. Gas adsorption properties of SIFSIX-1-Cu and the MOMs reported herein.

MOM	SIFSIX-1-Cu	TIFSIX-1-Cu	SNIFSIX-1-Cu
Empirical formula	$[Cu(SiF_6)(bipy)_2]$	$[Cu(TiF_6)(bipy)_2]$	$[Cu(SnF_6)(bipy)_2]$
Pore volume (theoretical; cm^3/g)	0.683	0.696	0.636
BET surface area (m^2/g)	1468	1690	1523
BET surface area (m^2/cm^3)	1261	1457	1444
CO_2 uptake (1 atm, 298 K; cm^3/g)	115.2	106.3	93.9
CO_2 uptake (1 atm, 298 K; cm^3/cm^3)	99.0	91.6	89.0
CO_2 uptake (0.15 atm, 298 K; cm^3/g)	18.1	20.4	18.0
CO_2 uptake (0.15 atm, 298 K; cm^3/cm^3)	15.5	17.6	17.1
CO_2 Q_{st} (zero loading; kJ/mol)	26.5	26.6	26.4
CO_2/CH_4 relative uptake (1 atm, 298 K)	9.9	8.6	8.7
CO_2/N_2 relative uptake (1 atm, 298 K)	28.1	23.6	18.8
CO_2/CH_4 selectivity (50/50; 1 atm, 298 K)	10.6	11.2	12.1
CO_2/N_2 selectivity (10/90; 1 atm, 298 K)	26.5	29.5	21.9

Table S3. Gravimetric CO_2 uptake of selected MOMs at 298 K and 1 atm.

MOM	CO_2 Uptake @ 298 K, 1 atm (cm^3/g)	Reference
Mg_2(dobdc)	193.0	11
Co_2(dobdc)	169.0	12
Ni_2(dobdc)	160.0	12
Fe_2(dobdc)	159.0	13
[Cu(Me-4py-trz-ia)]	136.6	14
Cu-TDPAT	132.2	15
HKUST-1	126.0 (a)	16
Cu-TPBTM	118.5	17
SIFSIX-1-Cu	115.2	18
UTSA-20	112.0 (b)	19
Zn_2(dobdc)	109.8	20
PCN-26	109.1	21
Mg_2(dobpdc)	108.6	22
TIFSIX-1-Cu	106.3	This work

(a) 293 K, 1.1 atm; (b) 300 K.

11. Z. Bao, L. Yu, Q. Ren, X. Lu and S. Deng, *J. Colloid Interface Sci.*, 2011, **353**, 549.

12. A. O. z. r. Yazaydın, R. Q. Snurr, T. H. Park, K. Koh, J. Liu, M. D. LeVan, A. I. Benin, P. Jakubczak, M. Lanuza, D. B. Galloway, J. J. Low and R. R. Willis, *J. Am. Chem. Soc.*, 2009, **131**, 18198.

13. M. Märcz, R. E. Johnsen, P. D. C. Dietzel and H. Fjellvåg, *Micropor. Mesopor. Mat.*, 2012, **157**, 62.

14. D. Lässig, J. Lincke, J. Moellmer, C. Reichenbach, A. Moeller, R. Gläser, G. Kalies, K. A. Cychosz, M. Thommes, R. Staudt and H. Krautscheid, *Angew. Chem.*, 2011, **123**, 10528-10532.

15. B. Li, Z. Zhang, Y. Li, K. Yao, Y. Zhu, Z. Deng, F. Yang, X. Zhou, G. Li, H. Wu, N. Nijem, Y. J. Chabal, Z. Lai, Y. Han, Z. Shi, S. Feng and J. Li, *Angew. Chem. Int. Ed.*, 2012, **51**, 1412.

16. P. Aprea, D. Caputo, N. Gargiulo, F. Iucolano and F. Pepe, *J. Chem. Eng. Data*, 2010, **55**, 3655.

17. B. Zheng, J. Bai, J. Duan, L. Wojtas and M. J. Zaworotko, *J. Am. Chem. Soc.*, 2011, **133**, 748.

18. S. D. Burd, S. Ma, J. A. Perman, B. J. Sikora, R. Q. Snurr, P. K. Thallapally, J. Tian, L. Wojtas and M. J. Zaworotko, *J. Am. Chem. Soc.*, 2012, **134**, 3663.

19. Z. Guo, H. Wu, G. Srinivas, Y. Zhou, S. Xiang, Z. Chen, Y. Yang, W. Zhou, M. O'Keeffe and B. Chen, *Angew. Chem. Int. Ed.*, 2011, **50**, 3178.

20. A. R. Millward and O. M. Yaghi, *J. Am. Chem. Soc.*, 2005, **127**, 17998.

21. W. Zhuang, D. Yuan, D. Liu, C. Zhong, J.-R. Li and H. C. Zhou, *Chem. Mater.*, 2011, **24**, 18.

22. T. M. McDonald, W. R. Lee, J. A. Mason, B. M. Wiers, C. S. Hong and J. R. Long, *J. Am. Chem. Soc.*, 2012, **134**, 705.

Table S4. CO_2/CH_4 relative uptakes and CO_2 uptakes of MOMs reported in the literature at 298 K and 1 atm (Fig. 3 plot).

MOM	CO_2/CH_4 Relative Uptake	CO_2 Uptake (cm^3(STP)/g)	Reference
CUK-1	10.88	87.0	23
SIFSIX-1-Cu	9.90	115.2	24
SNIFSIX-1-Cu	8.70	93.9	This work
TIFSIX-1-Cu	8.60	106.3	This work
Mg_2(dobdc)	8.21	193.0	25
CD-MOF-2	7.73	58.0	26
UTSA-16	7.62(a)	102.5	27
$Cu(bpe)_2SiF_6$	6.26	62.1	24
iso1	6.25	28.0	28
MgH_6ODTMP	5.40 (b)	12.1	29
Cu-TDPAT	5.36	132.2	30
UTSA-20	5.31 (c)	112.0	31
CAU-1	4.83	87.0	32
NOTT-202	4.79(d)	31.6	33
SNU-50	4.71	80.0	34
ZIF-82	4.64	51.0	35
PCN-26	4.53	109.1	36
Cu_2(TCMBT)(bpp)(μ^3-OH)	4.48	44.8	37
UiO-66-NH_2	4.42	67.2	38
UiO-66-2,5-$(OMe)_2$	4.34	58.2	38
$Zn_4(OH)_2$(1,2,4-btc)$_2$	4.20 (e)	42.0	39
Cu(bdc-OH)	4.00 (a)	52.0	40
MIL-120	4.00 (b)	72.0	41
NOTT-140	3.96 (d)	93.0	42
PCN-80	3.90 (e)	61.1	43
ZIF-78	3.85	50.0	44
ZIF-81	3.80	38.0	44
UiO-66-NO_2	3.76	57.1	38
$Zn_5(bta)_6(tda)_2$	3.70 (e)	37.0	45
ZIF-68	3.60	36.0	44
ZIF-95	3.58	18.6	46
UiO-66	3.56	39.2	38
Cu_3(TerTri)$_2$(dabco)	3.56	32.0	47
ZIF-69	3.55	39.0	44
UiO-66-1,4-Naphthyl	3.51	34.7	38
SNU-21S	3.46	56.5	48
ZIF-79	3.30	33.0	44
SNU-21H	3.29	49.1	48
SNU-25	3.27	33.4	49
ZIF-100	3.19	20.0	46
Zn_3L2(4,4′-bipy)$_2$ (FIR-2)	3.18	35.0	50
MIL-101(Cr)	3.14 (f)	24.6	51
ZIF-70	3.11	28.0	44
Zn_2(ndc)$_2$(DPNI)	2.70	29.7	52
MOF-508b	2.57 (b)	40.3	53
SNU-77H	2.32	20.1	54
$Eu_2(TPO)_2$(HCOO)	1.52	31.8	55
$Y_2(TPO)_2$(HCOO)	1.41	43.4	55

(a) 296 K; (b) 303 K; (c) 300 K; (d) 293 K;(e) 295 K; (f) 313 K.

23. J. W. Yoon, S. H. Jhung, Y. K. Hwang, S. M. Humphrey, P. T. Wood and J. S. Chang, *Adv. Mater*., 2007, **19**, 1830.
24. S. D. Burd, S. Ma, J. A. Perman, B. J. Sikora, R. Q. Snurr, P. K. Thallapally, J. Tian, L. Wojtas and M. J. Zaworotko, *J. Am. Chem. Soc.*, 2012, **134**, 3663.
25. Z. Bao, L. Yu, Q. Ren, X. Lu and S. Deng, *J. Colloid Interface Sci*., 2011, **353**, 549.
26. R. S. Forgan, R. A. Smaldone, J. J. Gassensmith, H. Furukawa, D. B. Cordes, Q. Li, C. E. Wilmer, Y. Y. Botros, R. Q. Snurr, A. M. Z. Slawin and J. F. Stoddart, *J. Am. Chem. Soc*., 2011, **134**, 406.
27. S. Xiang, Y. He, Z. Zhang, H. Wu, W. Zhou, R. Krishna and B. Chen, *Nat.Commun.*, 2012, **3**, 954.
28. J. Ferrando-Soria, P. Serra-Crespo, M. de Lange, J. Gascon, F. Kapteijn, M. Julve, J. Cano, F. Lloret, J. Pasán, C. Ruiz-Pérez, Y. Journaux and E. Pardo, *J. Am. Chem. Soc*., 2012, **134**, 15301.
29. R. M. P. Colodrero, P. Olivera-Pastor, E. R. Losilla, D. Hernández-Alonso, M. A. G. Aranda, L. Leon-Reina, J. Rius, K. D. Demadis, B. Moreau, D. Villemin, M. Palomino, F. Rey and A. Cabeza, *Inorg. Chem*., 2012, **51**, 7689.
30. B. Li, Z. Zhang, Y. Li, K. Yao, Y. Zhu, Z. Deng, F. Yang, X. Zhou, G. Li, H. Wu, N. Nijem, Y. J. Chabal, Z. Lai, Y. Han, Z. Shi, S. Feng and J. Li, *Angew. Chem. Int. Ed*., 2012, **51**, 1412.
31. Z. Guo, H. Wu, G. Srinivas, Y. Zhou, S. Xiang, Z. Chen, Y. Yang, W. Zhou, M. O'Keeffe and B. Chen, *Angew. Chem. Int. Ed*., 2011, **50**, 3178.
32. X. Si, C. Jiao, F. Li, J. Zhang, S. Wang, S. Liu, Z. Li, L. Sun, F. Xu, Z. Gabelica and C. Schick, Energy & Environmental *Science*, 2011, **4**, 4522.
33. S. Yang, X. Lin, W. Lewis, M. Suyetin, E. Bichoutskaia, J. E. Parker, C. C. Tang, D. R. Allan, P. J. Rizkallah, P. Hubberstey, N. R. Champness, K. Mark Thomas, A. J. Blake and M. Schröder, *Nat. Mater*., 2012, **11**, 710.
34. T. K. Prasad, D. H. Hong and M. P. Suh, *Chem.– Eur. J*., 2010, **16**, 14043.
35. R. Banerjee, H. Furukawa, D. Britt, C. Knobler, M. O'Keeffe and O. M. Yaghi, *J. Am. Chem. Soc*., 2009, **131**, 3875.
36. W. Zhuang, D. Yuan, D. Liu, C. Zhong, J. R. Li and H. C. Zhou, *Chem. Mater*., 2011, **24**, 18.
37. Z. Lu, H. Xing, R. Sun, J. Bai, B. Zheng and Y. Li, *Cryst. Growth Des*., 2012, **12**, 1081.
38. G. Cmarik, M. Kim, S. M. Cohen and K. S. Walton, *Langmuir*, 2012, doi: 10.1021/la3035352.
39. Z. Zhang, S. Xiang, X. Rao, Q. Zheng, F. R. Fronczek, G. Qian and B. Chen, *Chem. Commun*., 2010, **46**, 7205.
40. Z. Chen, S. Xiang, H. D. Arman, P. Li, S. Tidrow, D. Zhao and B. Chen, *Eur. J. Inorg. Chem*., 2010, **2010**, 3745.
41. C. Volkringer, T. Loiseau, M. Haouas, F. Taulelle, D. Popov, M. Burghammer, C. Riekel, C. Zlotea, F. Cuevas, M. Latroche, D. Phanon, C. Knöfelv, P. L. Llewellyn and G. Férey, *Chem. Mater.,* 2009, **21**, 5783.
42. C. Tan, S. Yang, N. R. Champness, X. Lin, A. J. Blake, W. Lewis and M. Schroder, *Chem. Commun*., 2011, **47**, 4487.
43. W. Lu, D. Yuan, T. A. Makal, J. R. Li and H. C. Zhou, *Angew. Chem. Int. Ed*., 2012, **51**, 1580.
44. R. Banerjee, H. Furukawa, D. Britt, C. Knobler, M. O'Keeffe and O. M. Yaghi, *J. Am. Chem. Soc*., 2009, **131**, 3875.
45. Z. Zhang, S. Xiang, Y. S. Chen, S. Ma, Y. Lee, T. Phely-Bobin and B. Chen, *Inorg. Chem*., 2010, **49**, 8444.
46. B. Wang, A. P. Cote, H. Furukawa, M. O'Keeffe and O. M. Yaghi, *Nature*, 2008, **453**, 207.
47. C. Hou, Q. Liu, J. Fan, Y. Zhao, P. Wang and W. Y. Sun, *Inorg. Chem.,* 2012, **51**, 8402.
48. T. K. Kim and M. P. Suh, *Chem. Commun*., 2011, **47**, 4258.
49. Y. E. Cheon, J. Park and M. P. Suh, *Chem. Commun.,* 2009, 5436.
50. Y. X. Tan, Y. P. He and J. Zhang, *Cryst. Growth Des.,* 2012, **12**, 2468.
51. P. Chowdhury, C. Bikkina and S. Gumma, *J. Phys. Chem. C*, 2009, **113**, 6616.
52. Y.-S. Bae, K. L. Mulfort, H. Frost, P. Ryan, S. Punnathanam, L. J. Broadbelt, J. T. Hupp and R. Q. Snurr, *Langmuir*, 2008, **24**, 8592.
53. L. Bastin, P. S. Barcia, E. J. Hurtado, J. A. C. Silva, A. E. Rodrigues and B. Chen, *J. Phys. Chem. C*, 2008, **112**, 1575.
54. H. J. Park, D. W. Lim, W. S. Yang, T. R. Oh and M. P. Suh,*Chem.– Eur. J*., 2011, **17**, 7251.
55. Z. J. Lin, Z. Yang, T. F. Liu, Y. B. Huang and R. Cao, *Inorg. Chem*., 2012, **51**, 1813.

Table S5. 50/50 CO_2/CH_4 IAST selectivities of selected MOMs at 298 K and 1 atm.

MOM	Selectivity	Reference
ZIF-78	10	56, 57
ZIF-8	1.32	58
ZIF-82	9.8[a]	56
ZIF-95	4.3[a]	59
MOF-5	2.3	60
UMCM-1	1.82	58
MIL-53(Al)	2.30	58
MOF-177	0.89	58
$Zn(bdc)(dabco)_{0.5}$	3.4[b]	61
HKUST-1	~8	57, 62
MIL-101(Cr)	~12	57, 62

[a] Henry's Law selectivity; [b] at 294 K.

56. R. Banerjee, H. Furukawa, D. Britt, C. Knobler, M. O'Keeffe and O. M. Yaghi, *J. Am. Chem. Soc.*, 2009, **131**, 3875.
57. S. Xiang, Y. He, Z. Zhang, H. Wu, W. Zhou, R. Krishna and B. Chen, *Nat. Commun.*, 2012, **3**, 954.
58. Z. Xiang, X. Peng, X. Cheng, X. Li and D. Cao, *J. Phys. Chem. C*, 2011, **115**, 19864.
59. B. Wang, A. P. Cote, H. Furukawa, M. O'Keeffe and O. M. Yaghi, *Nature*, 2008, **453**, 207.
60. J. M. Simmons, H. Wu, W. Zhou and T. Yildirim, *Energy Environ. Sci.*, 2011, **4**, 2177.
61. P. Mishra, S. Mekala, F. Dreisbach, B. Mandal and S. Gumma, *Sep. Purif. Technol.*, 2012, **94**, 124.
62. P. Chowdhury, S. Mekala, F. Dreisbach and S. Gumma, *Micropor. Mesopor. Mat.*, 2012, **152**, 246.

Supplementary Data Figures

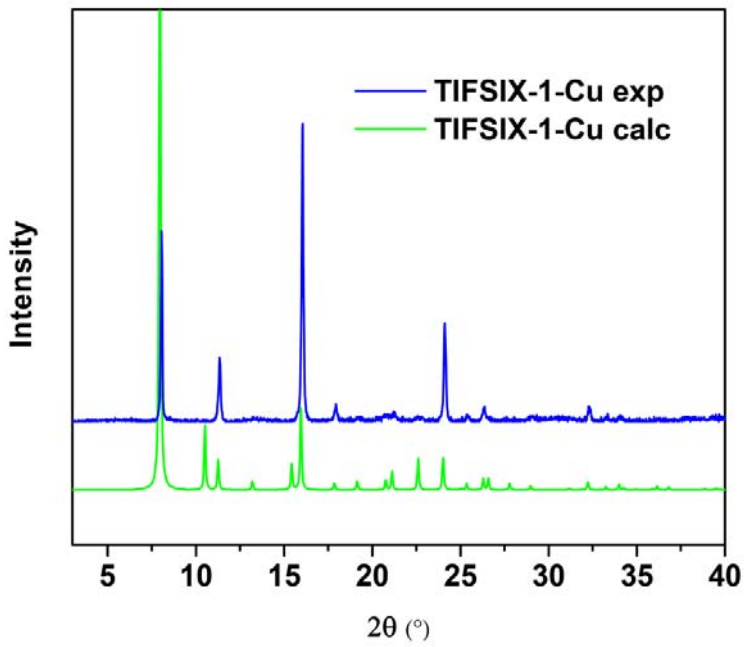

Fig. S1. Experimental and calculated PXRD patterns for **TIFSIX-1-Cu**.

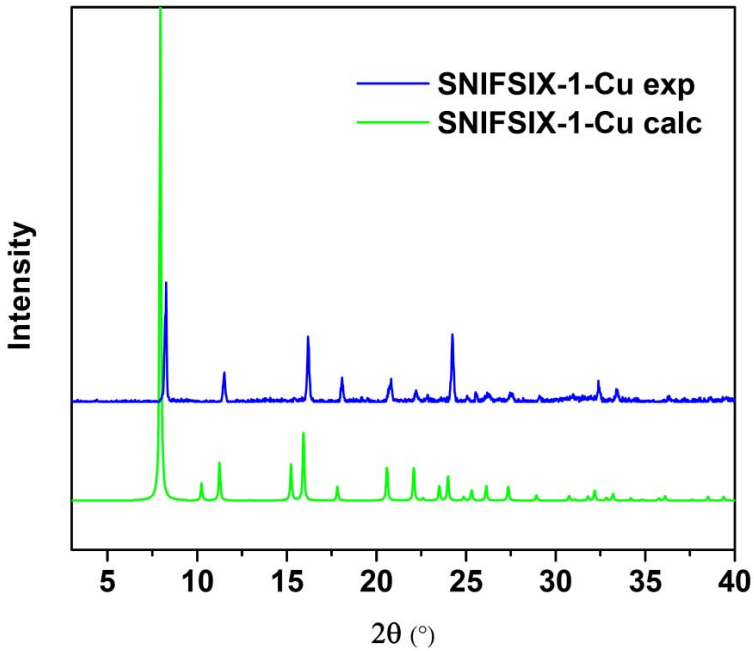

Fig. S2. Experimental and calculated PXRD patterns for **SNIFSIX-1-Cu**.

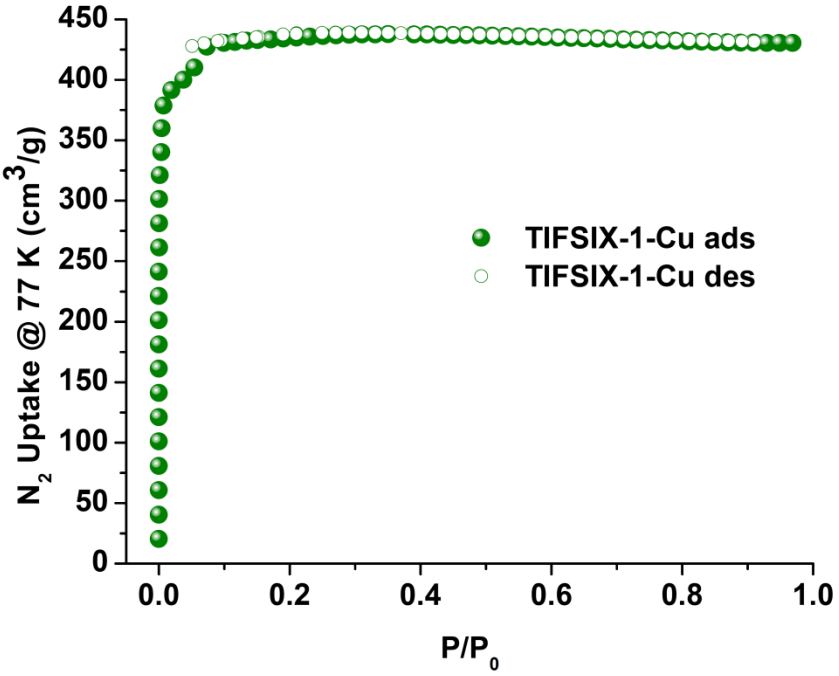

Fig. S3. N_2 isotherm at 77 K for **TIFSIX-1-Cu**.

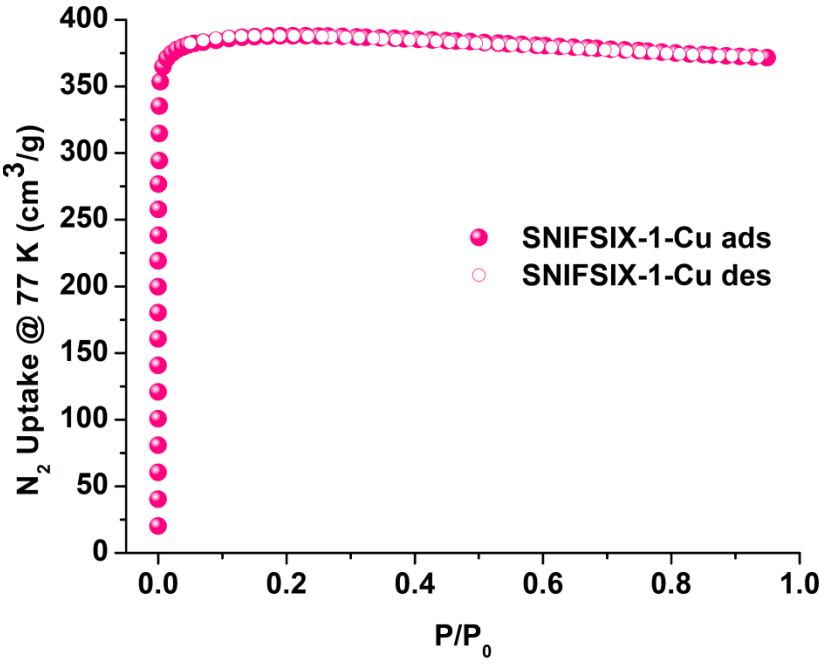

Fig. S4. N_2 isotherm at 77 K for **SNIFSIX-1-Cu**.

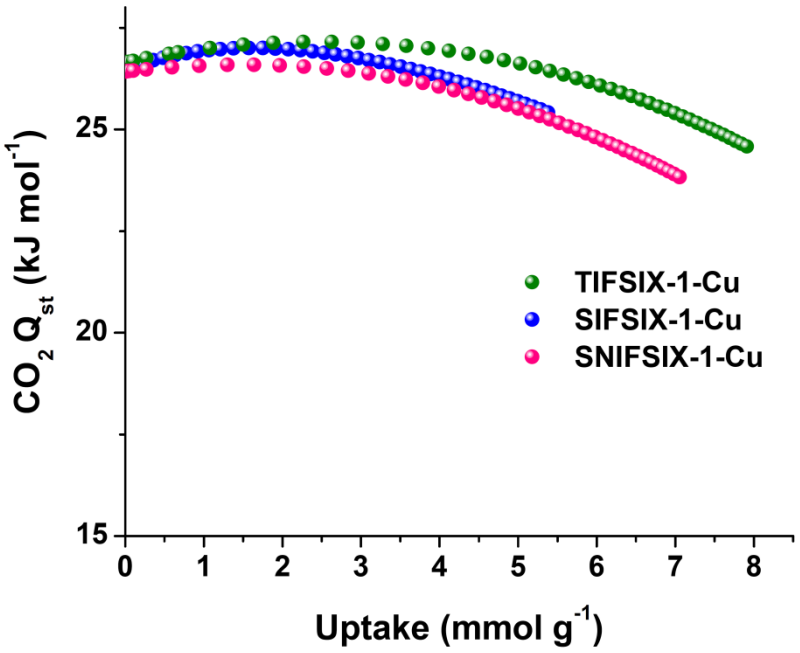

Fig. S5. CO_2 Q_{st} for **TIFSIX-1-Cu**, **SIFSIX-1-Cu**, and **SNIFSIX-1-Cu** determined by the virial method.

Modeling Summary

Modeling studies were performed to investigate the gas adsorption behavior in **SIFSIX-1-Cu**, **TIFSIX-1-Cu**, and **SNIFSIX-1-Cu**. Highly accurate and transferable CO_2, CH_4, and N_2 potentials were developed using a previously described fitting procedure.[63,64] Simulation parameters including atomic point partial charges, repulsion/dispersion parameters, and atomic point polarizabilities were also developed according to previous considerations.[65-68] Grand canonical Monte Carlo (GCMC) simulations[69] were able to predict the primary and secondary CO_2 adsorption sites based upon both binding energy and the magnitude of the dipole induced in CO_2. In all three MOMs, this interaction occurs between the carbon atom of CO_2 and the equatorial fluorines of the MF_6^{2-} (M = Si, Ti, Sn) moieties (Fig. S6). Further, comparison of the radial distribution functions, dipole distributions, and polarizability data of **TIFSIX-1-Cu** and **SIFSIX-1-Cu** (described below) are consistent with an enhanced framework-CO_2 interaction in the former due to the substitution of Si^{4+} with Ti^{4+}. Full details concerning modeling of the gas adsorption and separation mechanisms in these compounds will be described in a future manuscript.

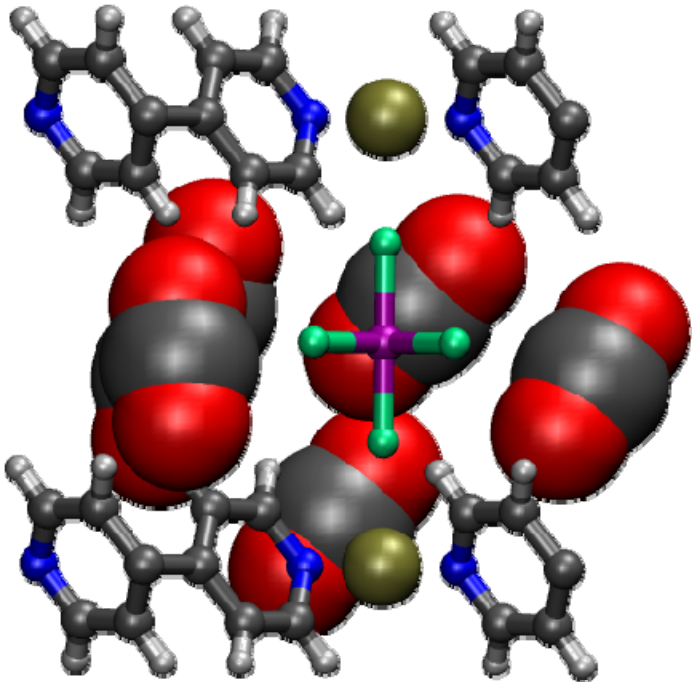

Fig. S6. Snapshot of the primary CO_2 binding site in **TIFSIX-1-Cu** determined from modeling studies. Atom colors: C = gray, H = white, O = red, N = blue, F = green, Cu = tan, Ti = violet.

Radial Distribution Function and Dipole Distribution

Examination of the radial distribution functions, g(r), of CO_2 molecules <11 Å from the pillaring metal in **SIFSIX-1-Cu** and **TIFSIX-1-Cu** reveals maxima at ca. 4.55 Å and 3.95 Å, respectively (Fig. S7). These peaks correspond to the closest interaction between the carbon atom of CO_2 and the equatorial fluorines

of the MF_6^{2-} pillars (Fig. S6). The smaller CO_2-M distance observed for **TIFSIX-1-Cu** signifies a stronger electrostatic attraction between the pillar and CO_2 in this variant compared to **SIFSIX-1-Cu**. The area under the 3.95 Å radial distribution peak in **TIFSIX-1-Cu** relative to that of the 4.55 Å peak in **SIFSIX-1-Cu** indicates that there is a larger population of CO_2 molecules interacting with the equatorial fluorines in the former. The distances between the equatorial fluorine atom and the carbon atom of the closest sorbed CO_2 were found to be 2.103 Å in **TIFSIX-1-Cu** and 2.850 Å in **SIFSIX-1-Cu**.

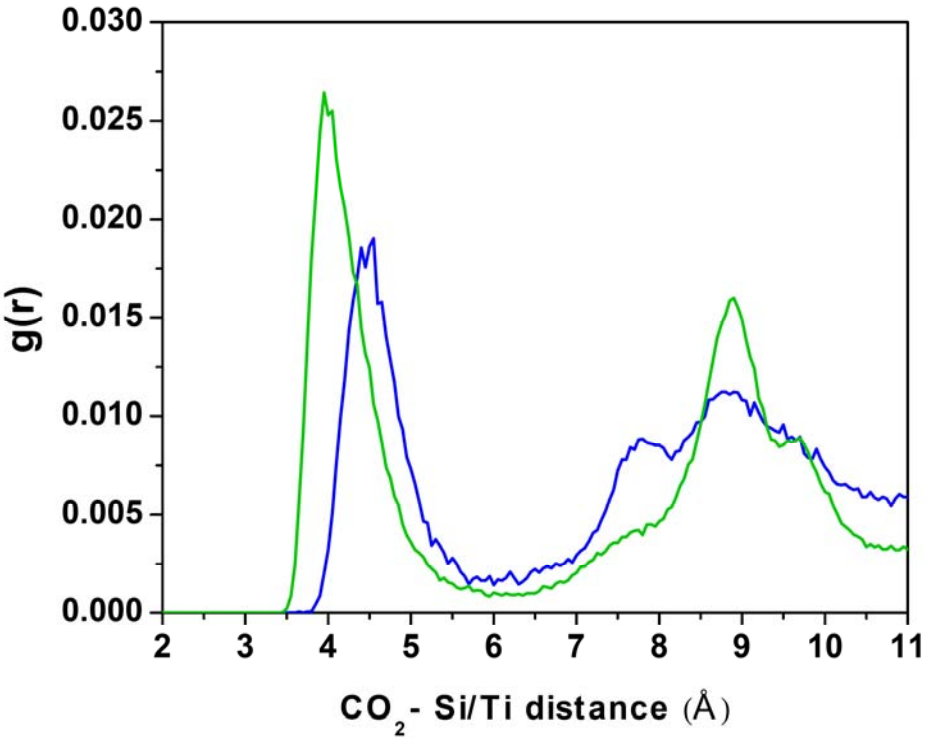

Fig. S7. The radial distribution functions of CO_2 molecules about the Si/Ti atoms in **SIFSIX-1-Cu** (blue) and **TIFSIX-1-Cu** (green) observed from simulations of CO_2 adsorption at 298 K and 1.0 atm.

Further insight into the favored CO_2 adsorption sites for **SIFSIX-1-Cu** and **TIFSIX-1-Cu** was obtained through molecular simulation studies involving explicit polarization. Similar methods were employed previously for H_2 adsorption in highly polar MOFs such as In-*soc*-MOF and PCN-61.[65,68] The normalized distribution of induced dipoles for CO_2 molecules adsorbed in the pores of **SIFSIX-1-Cu** and **TIFSIX-1-Cu** reveals two distinct peaks corresponding to different regions of sorbate occupancy (Fig. **S**8). For **TIFSIX-1-Cu**, the high dipole peak from 0.40 to 0.60 D correlates to the interaction between CO_2 and the equatorial fluorine atoms of the TiF_6^{2-} groups (i.e. the primary adsorption site; Fig. S9, red shaded areas). The primary adsorption site is similar in the case of **SIFSIX-1-Cu**, though the dipole magnitudes are slightly lower (0.30 to 0.50 D). This data indicates that **TIFSIX-1-Cu** induces higher dipoles on CO_2 molecules upon adsorption due to the greater polarizability of Ti^{4+} relative to Si^{4+}. A peak from 0.05 to 0.15 D was also observed for both compounds which corresponds to a secondary adsorption site (Fig. S9,

cyan shaded areas) whereby CO_2 coordinates to the CO_2 molecules that are already occupying the primary adsorption site.

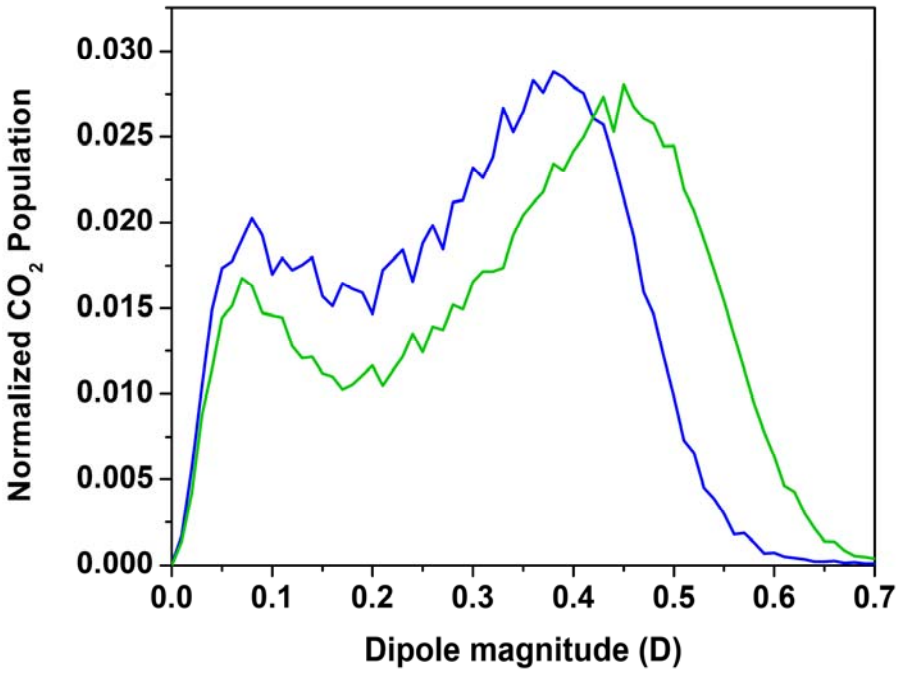

Fig. S8. The normalized CO_2 dipole distribution from simulations of CO_2 adsorption in **SIFSIX-1-Cu** (blue) and **TIFSIX-1-Cu** (green) at 298 K and 1.0 atm.

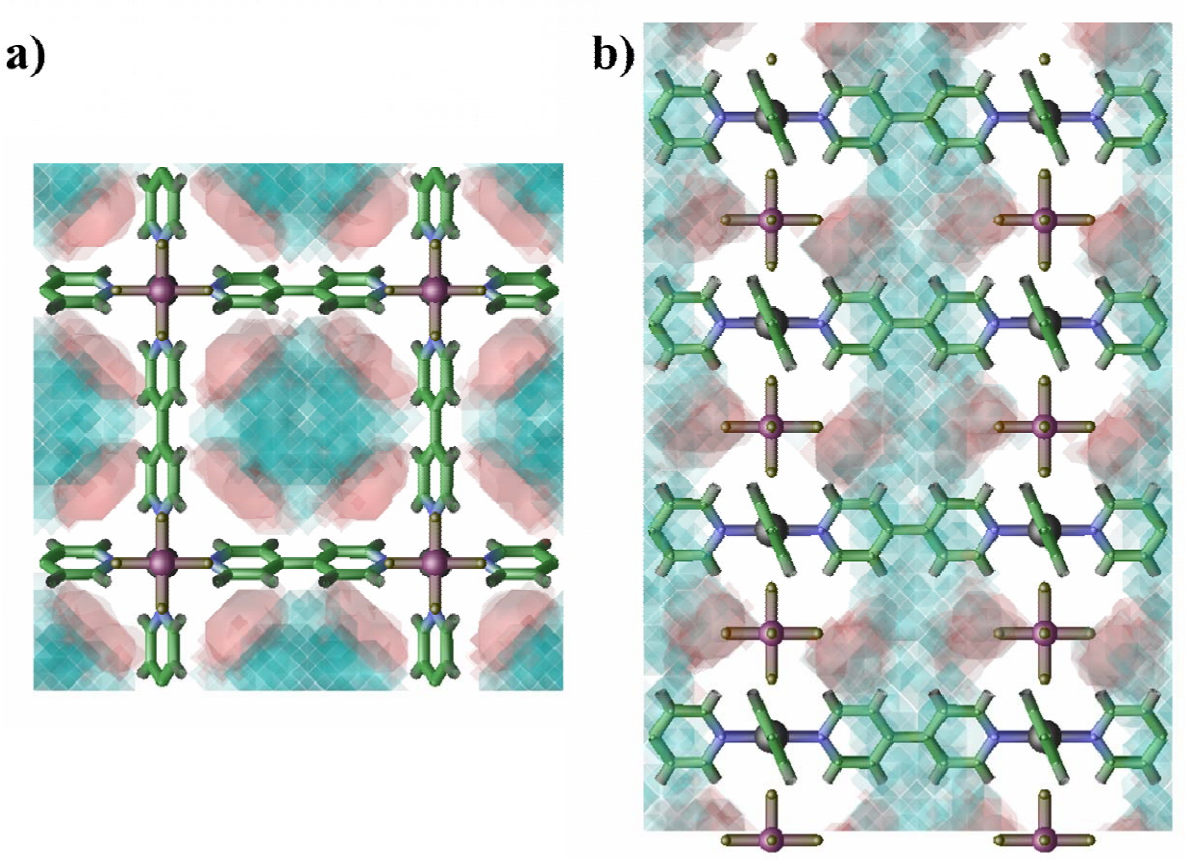

Fig. S9. Three-dimensional histograms showing the sites of CO_2 adsorption in **SIFSIX-1-Cu/TIFSIX-1-Cu**: **(a)** c axis view; **(b)** a/b axis view. Red regions correspond to CO_2 adsorbed at the primary dipole site, while cyan regions correspond to the CO_2 molecules adsorbed at the secondary dipole site.

Polarizability Calculations

To determine the atomic point polarizabilities of Si^{4+} and Ti^{4+}, polarizability tensors of gas phase SiF_6^{2-} and TiF_6^{2-} were calculated by restricted Hartree-Fock methods with the aug-cc-pVDZ basis set using Q-Chem code.[70] The polarizability for Si^{4+}/Ti^{4+} was then determined by fitting the molecular polarizability tensor for SiF_6^{2-}/TiF_6^{2-}, calculated using the Thole-Applequist model,[71-73] to the Hartree-Fock polarizability tensor form. For this calculation, all F atoms were assigned the fluorine polarizability value as parameterized by van Duijnen et al.[74] Following this procedure, the polarizabilities of Si^{4+} and Ti^{4+} were calculated to be 2.1330 $Å^3$ and 3.2428 $Å^3$, respectively. These polarizabilities reinforce the assertion that the equatorial fluorines possess greater electron density when bound to Ti^{4+} than to Si^{4+}, leading in turn to enhanced interaction with CO_2.

63. J. L. Belof, A. C. Stern and B. Space, *J. Chem. Theory Comput*., 2008, **4**, 1332.
64. K. McLaughlin, C. R. Cioce, J. L. Belof and B. Space, *J. Chem. Phys*., 2012, **136**, 194302.
65. J. L. Belof, A. C. Stern, M. Eddaoudi and B. Space, *J. Am. Chem. Soc*., 2007, **129**, 15202.

66. J. L. Belof, A. C. Stern and B. Space, *J. Phys. Chem. C*, 2009, **113**, 9316.
67. A. C. Stern, J. L. Belof, M. Eddaoudi and B. Space, *J. Chem. Phys*., 2012, **136**, 034705.
68. K. A. Forrest, T. Pham, K. McLaughlin, J. L. Belof, A. C. Stern, M. J. Zaworotko and B. Space, *J. Phys. Chem. C*, 2012, **116**, 15538.
69. N. Metropolis, A. W. Rosenbluth, M. N. Rosenbluth, A. H. Teller and E. Teller, *Phys. Lett. B*, 1953, **21**, 1087.
70. Y. Shao et al. *PCCP*, 2006, **8**, 3172.
71. J. Applequist, J. R. Carl and K. K. Fung, *J. Am. Chem. Soc.*, 1972, **94**, 2952.
72. B. T. Thole, *Chem. Phys.*, 1981, **59**, 341.
73. K. A. Bode and J. Applequist, *J. Phys. Chem.*, 1996, **100**, 17820.
74. P. T. van Duijnen and M. Swart, *J. Phys. Chem. A*, 1998, **102**, 2399.

Ideal Adsorbed Solution Theory (IAST)

In order to predict binary mixture adsorption in **SIFSIX-1-Cu**, **TIFSIX-1-Cu**, and **SNIFSIX-1-Cu**, the respective single-component CO_2, CH_4, and N_2 adsorption isotherms were first fit to the dual-site Langmuir-Freundlich equation[75]:

$$n = \frac{n_{m1} b_1 P^{\left(\frac{1}{t_1}\right)}}{1 + b_1 P^{\left(\frac{1}{t_1}\right)}} + \frac{n_{m2} b_2 P^{\left(\frac{1}{t_2}\right)}}{1 + b_2 P^{\left(\frac{1}{t_2}\right)}}$$

In this equation, n is the amount adsorbed per mass of adsorbent (in mol/kg), P is the total pressure (in kPa) of the bulk gas at equilibrium with the adsorbed phase, n_{m1} and n_{m2} are the saturation uptakes (in mol/kg) for sites 1 and 2, b_1 and b_2 are the affinity coefficients (in kPa^{-1}) for sites 1 and 2, and t_1 and t_2 are the heterogeneity factors for sites 1 and 2. All isotherms were fitted with $R^2 \geq 0.9999$. Indeed, this equation has been used to fit isotherm data for a variety of MOMs.[76-81] The fitted isotherm parameters were applied to perform the necessary integrations according to IAST.[82,83] Afterwards, the selectivity for component i relative to component j was calculated by the following equation:

$$S_{i/j} = \frac{x_i y_j}{x_j y_i}$$

Here, x_i and y_i are the mole fractions of component i in the adsorbed and bulk phases, respectively.

75. R. T. Yang, *Gas Separation by Adsorption Processes*, Imperial College Press, 1986.
76. V. Goetz, O. Pupier and A. Guillot, *Adsorption,* 2006, **12**, 55.
77. R. Babarao, Z. Hu, J. Jiang, S. Chempath, and S. I. Sandler, *Langmuir*, 2007, **23**, 659.
78. Y. S. Bae, K. L. Mulfort, H. Frost, P. Ryan, S. Punnathanam, L. J. Broadbelt, J. T. Hupp and R. Q. Snurr, *Langmuir,* 2008, **24**, 8592.
79. B. Zheng, J. Bai, J. Duan, L. Wojtas and M. J. Zaworotko, *J. Am. Chem. Soc*., 2011, **133**, 748.
80. S. D. Burd, S. Ma, J. A. Perman, B. J. Sikora, R. Q. Snurr, P. K. Thallapally, J. Tian, L. Wojtas and M. J. Zaworotko, *J. Am. Chem. Soc*., 2012, **134**, 3663.
81. Z. Zhang, Z. Li and J. Li, *Langmuir*,2012, **28**, 12122.
82. A. L. Myers and J. M. Prausnitz, *AIChE Journal,* 1965, **11**, 121.
83. A. J. Kidnay and A. L. Myers, *AIChE Journal,* 1966, **12**, 981.

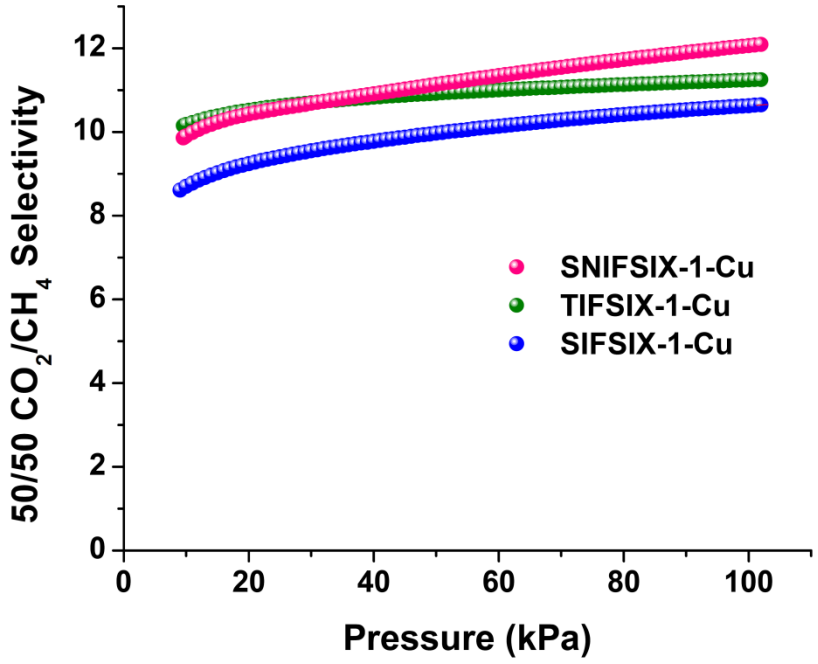

Fig. S10. 50/50 CO_2/CH_4 IAST selectivities of **TIFSIX-1-Cu**, **SIFSIX-1-Cu**, and **SNIFSIX-1-Cu** at 298 K.

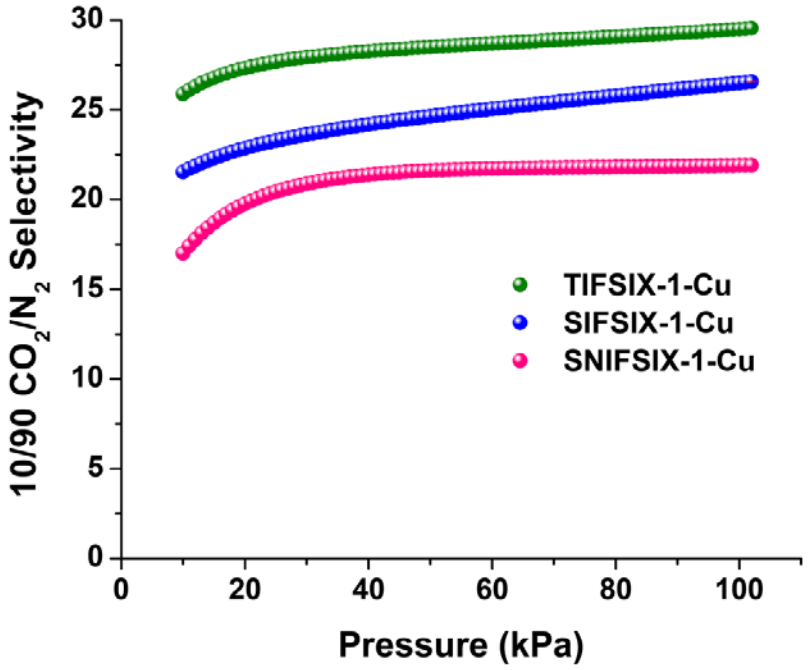

Fig. S11. 10/90 CO_2/N_2 IAST selectivities of **TIFSIX-1-Cu**, **SIFSIX-1-Cu**, and **SNIFSIX-1-Cu** at 298 K.